



# Clinical ultrasound image standardization using histogram specification

Rahul Roy<sup>a</sup>, Susmita Ghosh<sup>c</sup>, Ashish Ghosh<sup>b,\*</sup>

<sup>a</sup> Department of Computer Science and Engineering, National Institute of Science and Technology, Berhampur, India

<sup>b</sup> Machine Intelligence Unit, Indian Statistical Institute, Kolkata 700108, India

<sup>c</sup> Department of Computer Science and Engineering, Jadavpur University, Kolkata, India

## ARTICLE INFO

### Keywords:

Clinical ultrasound images  
Histogram specification  
Image standardization

## ABSTRACT

This article presents a novel ultrasound image standardization approach. This method aims to preserve the non-linear relationship in the echo-textures while ensuring the endurance in the transformed image. This is achieved by utilizing the concept of histogram specification. A reference cumulative distribution function (CDF) of a considered distribution is used to process the test images. Initially, the shape and scale parameter of the distribution are estimated for each type of echo-texture from the reference ultrasound images of a particular organ. These parameters are used to estimate the prototype parameter set. The obtained prototype parameter set, along with a distribution function, is then used to construct a reference CDF. This CDF, in turn, is used as a transfer function in the histogram specification technique for standardizing the given input image. The efficiency and stability of the proposed approach are investigated and compared with the linear scaling technique. Four measures are used to evaluate the algorithms on three data sets. The results show that the proposed approach provides better standardization of images and is invariant to the gain of the scanning device as opposed to linear scaling.

## 1. Introduction

Ultrasound image scanning suffers from a different source of intensity variations [1,2]. One such variation in intensity range occurs due to the non-uniform pressure applied on the transducer during scanning. The transducer is a hand-held device, and the amount of pressure applied by practitioners on the transducers cannot be uniform. This non-uniformity of pressure turns out to be a source of intensity range variation among each instance of scanned images for the same organ despite being scanned with the same device. The other source of variation in the intensities in the images is due to the difference in operating frequency of the devices and gain used during scanning for different individuals. These sources of variability in the images possess a significant challenge in the design of automated segmentation and classification system for the extraction of structures and identification of anomalies in the organs [3]. Moreover, they are a significant source of a hindrance to the computation of indicators for quantitative analysis [4,5].

The problem of standardization of ultrasound images is ill-studied in the field of ultrasound imaging research. Eltarozzy et al. [6] was the first to introduce a linear scaling mechanism for the standardization of ultrasound images and study its effect on the diagnosis of bifurcation plaque. Loizou et al. [7,8] showed that de-speckling followed by standardization provides a better segmentation of structures of the carotid

artery and have used the same linear scaling before segmentation of carotid artery structures from ultrasound images. Linear scaling scales the intensities without taking into consideration the distribution of the echo-textures (gray shades). It results in the loss of the actual reflective information of the organ. It motivated us to design a mechanism for ultrasound image standardization, which preserves the distribution of the echo-textures in the ultrasound images such that there is no loss of reflectivity of the organ. The approach performs the standardization by matching the histogram of the intensity distribution concerning considered distribution that can best characterize the ultrasound images. Histogram specification notion is used to build the model for standardization [9] i.e., a prototype of shape and scale parameter set of the considered distribution is estimated from the representative images. This parameter set is used for building the cumulative distribution function. The obtained CDF act as the transfer function for image standardization. It is assumed that the images follow mixture distribution. Thus for each kind of echo-texture, the prototype parameter set (shape and scale parameter) is estimated.

Initially, the intensity levels are grouped in different categories of echo-textures. It is assumed that three kinds of echo-textures are present in ultrasound images. Grouping is carried out using fuzzy C-means clustering [10]. The use of fuzzy C-means helps to form

\* Corresponding author.

E-mail addresses: [rahulroy@nist.edu](mailto:rahulroy@nist.edu) (R. Roy), [susmita.ghoshde@jadavpuruniversity.in](mailto:susmita.ghoshde@jadavpuruniversity.in) (S. Ghosh), [ash@isical.ac.in](mailto:ash@isical.ac.in) (A. Ghosh).

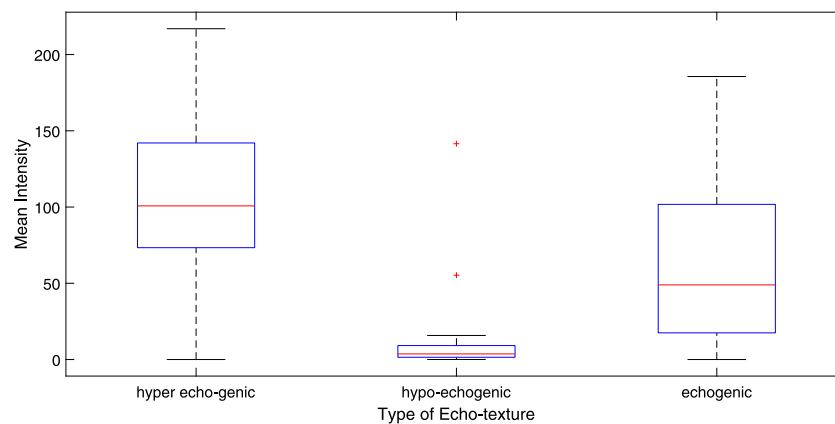


Fig. 1. Five number summary plot for mean intensity of different type echo-textures.

soft clusters where all  $L$  levels of intensities belong to every echo-texture with some degree of belonging [11,12]. The use of the degree of belonging for each echo-texture preserves the contribution of the distribution while highlighting a particular echo-texture and suppressing others. It helps in the proper estimation of the parameters for a particular echo-texture. In the second step, the scale and shape parameters of the assumed distribution function are estimated for each kind of echo-texture from the representative image. This shape and scale parameters taken together form a parameter set representing an image. It is noteworthy that the representative image set comprises images of the same organ from a particular angle of view. After that, a prototype parameter set is computed to the obtained parameters for calculating the cumulative distribution function (CDF). We estimate the parameters from the representative images and find a prototype parameter instead of selecting or averaging over the representative images for estimating the parameter of the distribution. Averaging of the representative image would be difficult due to the varying size of the image and varying angle of orientation of scanning, and the prototype image would not generalize the reference CDF. The obtained prototype parameters are plugged into the distribution function to form the CDF that acts as a transfer function for histogram specification. Finally, a new image is transformed using the obtained transfer function and the histogram specification algorithm. Two distribution functions, namely Nakagami [13] and generalized gamma [14] are considered in this experiment.

The main advantage of the proposed approach is that it preserves the non-uniform distribution of the echo-textures. This act, in turn, preserves the characteristics of the echo-textures in the images. The method is scale-invariant as the CDF (for transformation) is computed on the prototype parameter set obtained from the parameter sets calculated from the representative images. It may be noted here that this methodology for non-linear image standardization is the first of its kind as per the best knowledge of the authors. Though we have shown the method for standardization of clinical ultrasound, however, this can be extended to other imagery with the proper choice of the underlying distribution for modeling the CDF of the image. Experiments are carried out on three datasets, namely, ultrasound images of the carotid artery, slices of the 3D ultrasound image of heart and thyroid. Quantitative analysis of the transformation process is made using four indices, namely speckle strength index, peak signal to noise ratio index, correlation preservation index, and entropy. The results obtained showed significant performance improvement over the existing techniques.

The rest of the article is organized as follows. Section 2 provides a description of the investigations on the echo-textures of ultrasound images. In Section 3, details of the proposed standardization strategy is provided. Experimental results and their analysis are given in Section 4. Finally, conclusion and future scope of work are presented in Section 5.

## 2. Investigation on echo-textures characteristics in ultrasound images

An investigation about the statistics of the echo-textures is carried out to establish the relationship among the echo-textures empirically. Three echo-texture patches are manually extracted from the carotid artery image dataset, and the mean of each patch is calculated. Five statistics of the computed means is shown using a boxplot in Fig. 1. Although the results of carotid artery images are presented in the article, similar experiments were performed on other datasets, and the results obtained showed similar trends. It is evident from the figure that the inter-quartile range of the mean of the hypo-echogenic echo-textures is small, and they tend to be close to the median value. However, the hyper-echogenic and echogenic echo-textures have a broader inter-quartile range and the median is close to the first quartile of the echo-textures' distribution. Thus it can be inferred that they have a skewed distribution.

Linear scaling of the image would not preserve the skewness of the echo-texture distribution. It would alter the intensity range of the organ in the image which otherwise is necessary to characterize the tissues of an organ for correct diagnosis.

## 3. Proposed methodology

In this work, a novel image standardization technique is developed. The intuition of the work is to form a transfer function with the CDF of a distribution using a prototype parameter set for each type of echo-texture. It characterizes the distribution of intensity for the echo-textures of an organ in an ultrasound image. The prototype parameter set is an exemplar/representative of the parameter sets, which are the shape and scale parameters of considered distribution that would be used as reference distribution for histogram matching. The CDF constructed using the prototype parameter set is used as a transfer function for histogram specification of the test image. The use of such a transformation would preserve the non-linear relationship of the echo-texture while standardizing the images.

The entire work is divided into two phases. In the first phase, distribution parameters are estimated for each representative image of the particular organ. It may be noted that the representative set includes the images of the organ under investigation from different subjects and scanned with the same or different types of ultrasound devices at a different instance of time. After that, in the subsequent phase, a histogram matching of the test image is done with the reference transfer function, i.e., the CDF function constructed by plugging in the representative parameters obtained during the estimation phase. The generalized gamma [14] and Nakagami [13] distributions are used in this connection for modeling echo-textures as they can mimic different kinds of distributions under different scattering conditions [15]. A detail block diagram of the work is shown in Fig. 2. The following subsections describe each of the modules in detail.

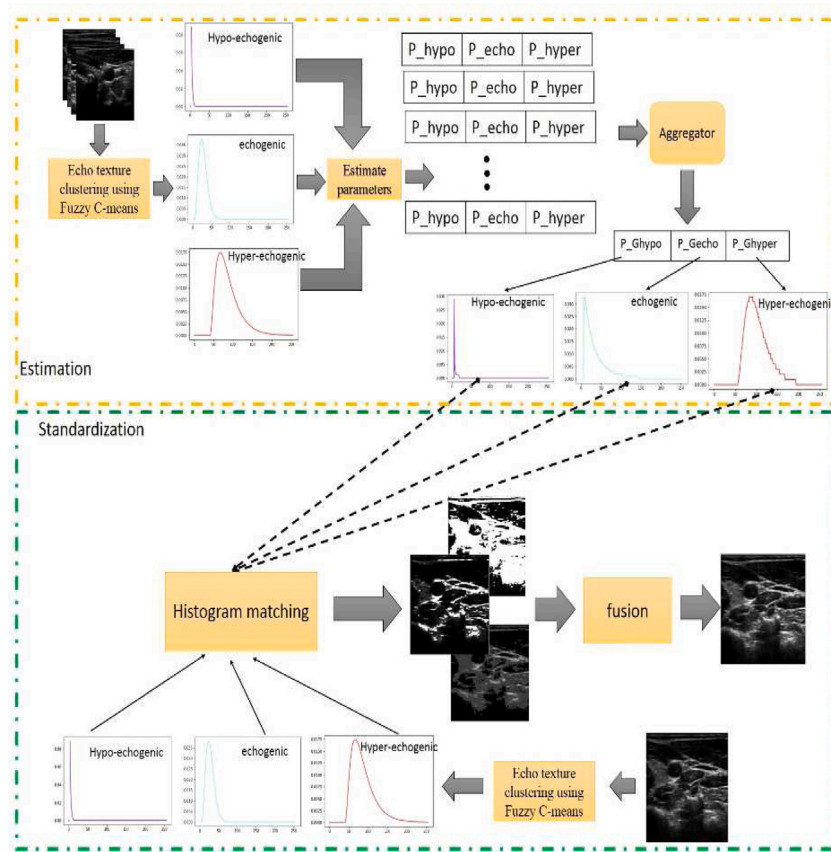


Fig. 2. Block diagram of the proposed approach.

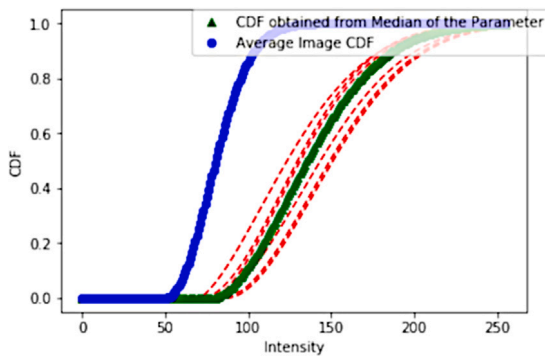


Fig. 3. CDFs constructed from the average of the representative images and from the average of the parameters obtained from each of the representative images. The blue colored line shows the CDF obtained from average image and the green line shows the CDF constructed with average parameter set obtained by aggregating the parameters from each image. The red line represents the parameter set computed from each representative image.

### 3.1. Echo-texture grouping

The organs provide different degrees of reflection, depending on the difference in impedance of the tissues of the organ. Thus, the image formed from these reflections has a mixture of different intensity levels. As per clinical ultrasound literature, these reflected echo-textures can be grouped into three categories, namely hypo-echogenic, echogenic (normal), and hyper-echogenic [16]. Hence, three clusters are considered for grouping the echo-texture. Nonetheless, this number may be varied depending on the need for finer granularity in the grouping of intensities in the image. The intensities in the image may have overlap

due to the partial volume effect during scanning. Furthermore, soft clustering of the intensity provides the degree of belonging to each cluster, which could be used for weighing the histogram of the intensities. It would help in focusing on a particular type of echo-texture among the available echo-textures without any loss in the continuity of the distribution function. Thus, we adopt the fuzzy C-means clustering [10] algorithm for grouping the intensities of the image.

An image  $I \in \mathbb{Z}$  have  $L$  level of intensities. Each intensity is assigned a membership of belonging to each of the three echo-textures. Thus, the membership  $\mu_j(l)$  for  $l \in L$  belonging to echo-texture  $j$  is computed as

$$\mu_j(l) = \frac{1}{\sum_{k=1}^3 \left( \frac{|l-c_j|}{|l-c_k|} \right)^{\frac{2}{\alpha-1}}} \quad (1)$$

where the cluster center  $c_j$  is calculated as

$$c_j = \frac{\sum_{l=1}^L (\mu_j(l))^\alpha l}{\sum_{l=1}^L (\mu_j(l))^\alpha} \quad (2)$$

Here  $\alpha$  is the fuzzifier.

Initially, the cluster center is set to a random value of  $l$ , and the membership is updated iteratively until the cluster center stabilizes. Each echo-texture distribution is obtained by weighing the histogram of the image intensity with the membership value of each intensity level. Scaling allows focusing on the intensities that describe the echo-texture.

### 3.2. Parameter estimation

The shape and scale parameters for the considered distribution of each echo-texture are estimated from the image. Consequently, they are used to form the exemplar set of parameters. The variability in size

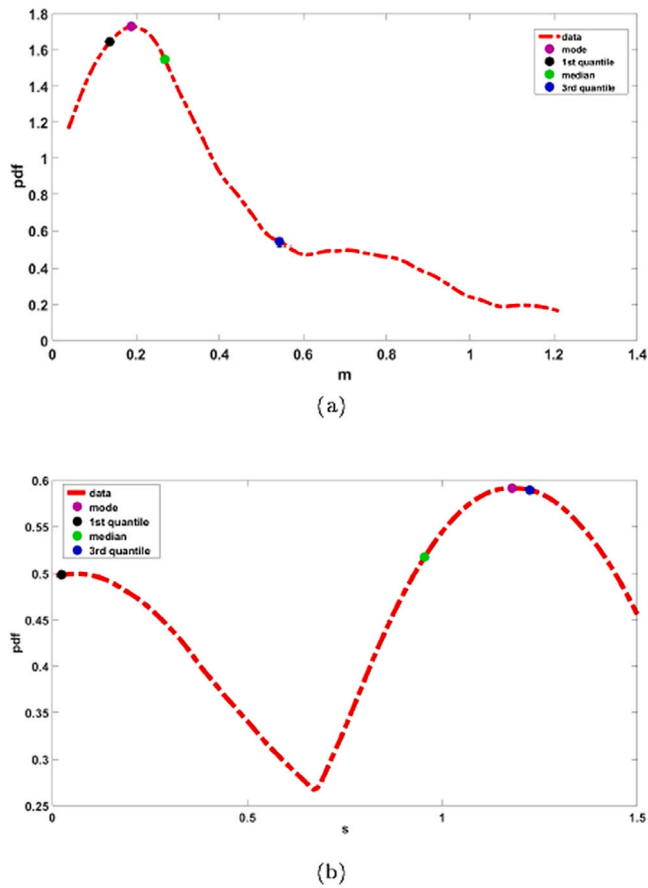


Fig. 4. Probability density function (PDF) plot for the estimated parameter (a)  $m$ , (b)  $s$  of hypo-echogenic echo-texture from the representative images..

and scale of the image and the organs causes hindrance in creating an aggregate representation of the image from which the parameters could be estimated. So, the parameters from each image are measured that helps to obtain scale and size invariant representation of the parameters. Another pitfall is that the average of the representative image set alters the intensity distribution. Thus, the CDF obtained has a different shape and scale as opposed to the CDF obtained from the prototype parameters set. This variation can be seen in Fig. 3. This variation in shape and scale would result in alteration in the reflective information of the organ. Thus, it is better to obtain the parameters estimated from the representative images and then form the prototype parameter set for the construction of the CDF.

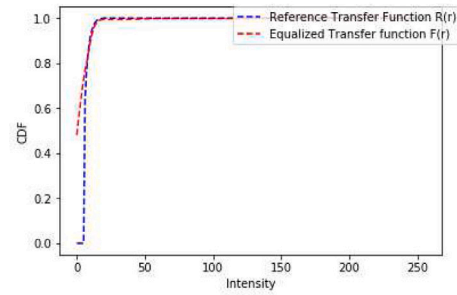
The parameters of each echo-texture distribution is estimated using the Maximum Likelihood Estimation (MLE) technique. Here, generalized gamma and Nakagami distributions are considered to model the echo-texture distributions. The probability distribution functions are defined by Eqs. (3) and (4)

$$p_L(l | s, m, \sigma) = \frac{s}{\Gamma(m)\sigma^{ms}} l^{ms-1} e^{-\left(\frac{l}{\sigma}\right)^s}, \quad l > 0 \quad (3)$$

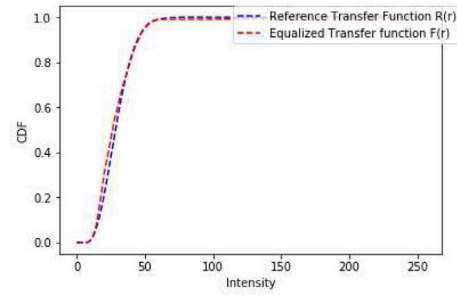
and

$$p_L(l | m, \sigma) = \frac{2m}{\Gamma(m)(2\sigma)^m} l^{2m-1} e^{-\frac{m}{2\sigma} l^2}, \quad l > 0. \quad (4)$$

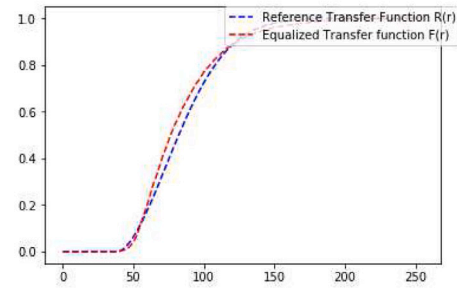
Here,  $s, m$ , and  $\sigma$  is the shape correction factor, shape, and scale parameter of the distributions, respectively.  $\Gamma$  represents the gamma function. It may be noted that the derivation of MLE for the generalized gamma distribution is shown in this article. Nonetheless, the MLE for estimation of parameters by considering Nakagami distribution can be derived similarly.



(a) Hypo-echogenic



(b) Echogenic



(c) Hyper-echogenic

Fig. 5. Reference transfer function alongwith the image normalized CDF for (a) hypo-echogenic, (b) echogenic and (c) hyper-echogenic echo-textures for ultrasound image.

The MLE for estimation of the parameters from  $n$  data points is done as

$$\mathcal{L}(m, s, \sigma) = \underset{m, s, \sigma}{\operatorname{argmax}} \prod_{i=1}^n p_L(l_i, s, m, \sigma); \quad (5)$$

$$\mathcal{L}(m, s, \sigma) = \underset{m, s, \sigma}{\operatorname{argmax}} \prod_{i=1}^n \frac{s}{\Gamma(m)\sigma^{ms}} l_i^{ms-1} e^{-\left(\frac{l_i}{\sigma}\right)^s}. \quad (6)$$

Applying negative of logarithm to Eq. (6) and simplifying it we get,

$$\begin{aligned} &\mathcal{L}(m, s, \sigma) \\ &= \underset{m, s, \sigma}{\operatorname{argmin}} \left( \sum_{i=1}^n \left( -ms \ln l_i + \left(\frac{l_i}{\sigma}\right)^s \right) + \left( \sum_{i=1}^n \ln l_i + n \ln \left( \frac{s}{\Gamma(m)\sigma^{ms}} \right) \right) \right). \end{aligned} \quad (7)$$

The last term in Eq. (7) produces a constant value and does not influence the optimization process. Thus, by ignoring the constant term, it can be written as

$$\mathcal{L}(m, s, \sigma) = \underset{m, s, \sigma}{\operatorname{argmin}} \left( \sum_{i=1}^n \left( -ms \ln l_i + \left(\frac{l_i}{\sigma}\right)^s \right) \right). \quad (8)$$

**Table 1**

Data set description.

Data set	Image size	No. of images	Representative set size	Test set size
Carotid	391 × 376	102	40	62
Thyroid	282 × 303	83	36	47
Cardiac	224 × 208	111	44	67

Here, estimation of the parameters (viz.,  $m, s, \sigma$ ) is done for all the three category echo-textures from each of the images in the representative set. All the parameters obtained from the representative images are used to obtain a prototype set of parameters that can provide an average description of the data. It may be noted that MLE needs an initialization of the parameters. So, we adopt the method given in [17] to initialize  $m_0$  as

$$m_0 = \frac{\mu(h_i^2)}{\nu(h_i^2)}; \tag{9}$$

where  $\mu$  and  $\nu$  are the mean and standard deviation of the histogram of each echo-texture. The scale parameter  $\sigma_0$  is set to the standard deviation of the histogram of the echo-texture and shape correction parameter  $s_0$  is set to 1.

As evident, the likelihood function is non-convex. Thus, the optimization of the task could result in the local optimum solution. So, we proceed with a heuristic approach defined in [18] along with MLE for estimation of the parameters. However, the constraint on the data used for evaluation must be greater than zero is explicitly asserted, such that there is no failure in the estimation. This assertion would result in a scale parameter to be higher than zero, and thus, there would be less chance of failure in the estimate.

An analysis of the estimated parameter distribution is carried out to find the near-optimal representative set that could generalize the distribution model for each category of echo-texture characteristics. It was observed that the distribution is skewed for most of the parameters, and in some cases, they are multi-modal (refer Figs. 4(a) and 4(b)). It is evident that for the left-skewed distribution of parameters, the mode would lie between the first quartile and the median, whereas for the right-skewed data, the mode is between the median and the third quartile [19]. In the case of a multi-modal distribution, the skewness would depend on the highest mode of the distribution. Thus, it can be seen that the choice of the median provides a near-maximum occurrence of the parameter value in both cases. Henceforth, the median value of parameters is considered to construct the prototype parameter set. This obtained prototype parameter set is finally used for building the CDF model to be used in the histogram matching as a reference model.

### 3.3. Histogram specification

Histogram specification [9] is used with this approach to transform the distribution of the image  $y$  with respect to the reference generalized model. Initially, the probability distribution  $p_r$  for each level  $r$  of the image is computed as

$$p_r = \frac{n_r}{n}, \quad r \in [0, L - 1] \tag{10}$$

Here  $n_r$  is the number of pixels with level  $r$  and  $n$  is the total number of pixels in the image. This probability distribution function PDF is used for constructing equalization transfer function (the CDF  $F(r)$ ) as

$$y_r = F(r) = (L - 1) \int_0^r p_r(w) dw. \tag{11}$$

The reference CDF,  $R(l)$  act as a specified transfer function for transforming the intensities. In this connection the CDF is generated by integrating Eq. (4) which gives

$$y_r^{ref} = R(l) = \int_0^l p_l(t, s, m, \sigma) dt = y_r. \tag{12}$$

or,

$$y_r^{ref} = R(l) = (L - 1) \frac{\gamma \left( m, \left( \frac{l}{\sigma} \right)^s \right)}{\Gamma(m)} - y_r. \tag{13}$$

To solve Eq. (13), the estimated prototype parameters, i.e.,  $m, s, \sigma$  are plugged and the value of  $y_r^{ref}$  is estimated. Computation of  $R^{-1}$  does not have a closed form, so an iterative approach is formulated by minimizing

$$l^* = \underset{l}{\operatorname{argmin}} R(l) = \underset{l}{\operatorname{argmin}} \left( \gamma \left( m, \left( \frac{l}{\sigma} \right)^s \right) - \frac{y_r \Gamma(m)}{L-1} \right). \tag{14}$$

This (Eq. (14)), actually means constructing a look up table between the input intensity level and output intensity level such that the two intensity levels have the same CDF value.

Fig. 5 shows the normalized transfer function of each type of echo-texture for an image and the reference transfer function (in this case the CDF) obtained by plugging in the prototype parameters to the generalized gamma distribution function. The obtained lookup table can be used for specification of the input histogram to obtain the standardized image.

The entire discussion is summarized in Algorithms 1 and 2.

---

#### Algorithm 1 Histogram Specification based Image Standardization: Estimation

---

```

for each image  $i$  in representative set  $T$  do
    Group the image into  $k$  clusters and obtain the membership of each intensity level
    Compute the histogram  $h$  of the image  $i$ 
    for each cluster  $C_i$  do
        Multiply the membership values corresponding to cluster  $C_i$  with histogram  $h$  to get  $h'$ 
        Create a data vector  $d$  from the histogram  $h'$ 
        Estimate the parameters using MLE with  $m_0, s_0, \sigma_0$  and  $d$ 
        Store the estimated parameters in  $P_i$ 
    end for
end for
 $P_r = \operatorname{median}$  of  $P$ ;
    
```

---



---

#### Algorithm 2 Histogram Specification based Image Standardization: Histogram Specification

---

```

Cluster the image  $y$  into  $k$  echo-textures;
Compute the histogram  $h$  for image  $y$ ;
for each echo-texture cluster  $i$  do
    Multiply the membership for cluster  $i$  with histogram  $h$  and form  $h'$ .
    Compute the CDF table for  $T_1$  from histogram  $h'$ ;
    Construct the reference CDF table  $T_2$  using the distribution function and the parameter  $P'_i$ ;
    Add to the lookup table  $T$  by matching each intensity level in  $T_1$  to  $T_2$  in the echotexture such that it satisfies Eq. (14);
end for
Compute  $Z$  using the lookup table  $T$  and  $y$ ;
    
```

---

Algorithm 1 summarizes the estimation of the reference parameter set  $P_r$  using the parameters estimated from echo-textures of each representative image. The estimated parameters are stored in  $P$ . It may be noted that in this case, we compute 12 parameters for the three echo-textures from each image. The median of the parameters in  $P$  is used to form the reference parameter set. Algorithm 2 provides the pseudocode for obtaining the lookup table  $T$  using the reference CDF and the new image CDF. The lookup table is formed by matching the CDF table  $T_1$  and  $T_2$  by satisfying the criterion mentioned in Eq. (14). This lookup table is used as a reference for transforming the image  $y$  to  $z$ .

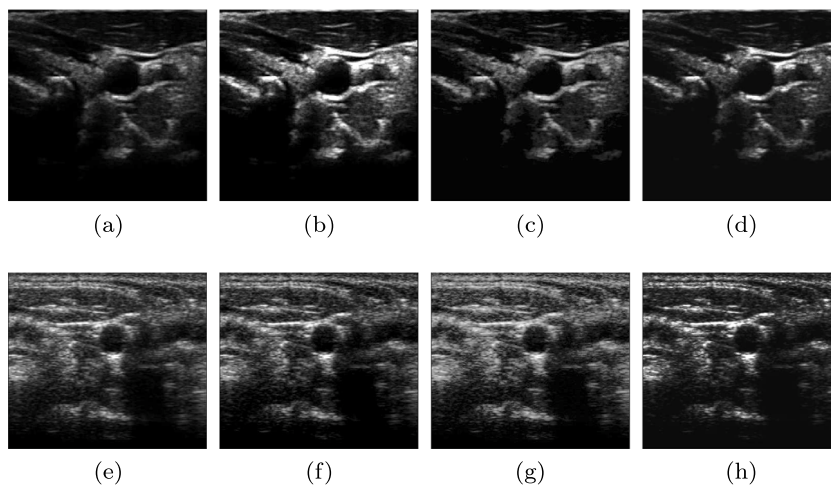


Fig. 6. (a) & (e) Original carotid sample image. Standardized images obtained by: (b) & (f) linear scaling, (d) & (g) Nakagami distribution based histogram specifications and (d) & (h) generalized gamma distribution based histogram specifications.

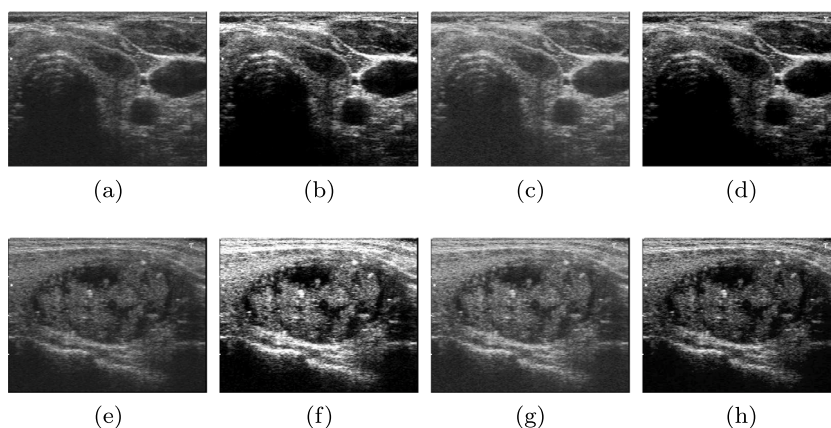


Fig. 7. (a) & (e) Original thyroid sample image. Standardized images obtained by: (b) & (f) linear scaling, (d) & (g) Nakagami distribution based histogram specifications and (d) & (h) generalized gamma distribution based histogram specifications.

**Table 2**  
Average measure computed from the transformed images obtained by different algorithms.

	Algorithms	SSI	PSNR index	CPI	Entropy
Carotid	Linear scaling	1.134692	0.968279	0.815449	3.765017
	Generalized gamma	0.981671	1.006161	0.857928	3.636084
	Nakagami	0.995816	0.966979	0.821769	3.632351
Thyroid	Linear scaling	1.700286	0.968709	0.920427	4.405153
	Generalized gamma	1.364173	0.969946	0.97443128	4.15665507
	Nakagami	0.932464	0.980919	0.94042	4.706737
Cardiac slice	Linear scaling	1.343727	0.943173	0.598651	2.714678
	Generalized gamma	1.192361	0.965244	0.616144	2.652373
	Nakagami	0.855534	0.960511	0.658417	3.042202

#### 4. Experimental results and analysis

Experiments are carried out on an Intel Core i7 3.40 GHz processor, with 16 GB RAM, Windows operating system, and Python programming environment. The measures used for testing were programmed in Matlab. Three image databases, viz., carotid artery data set [20,21], slices from the 3D ultrasound of heart from CETUS data set [22] and thyroid image data set [23] are used in the experiment. The details of the data set are provided in Table 1. Here, it is to be noted that we have ensured that the test set and representative image set are mutually exclusive.

The cumulative results of test images of each data set are reported in the article.

##### 4.1. Measures

The performance of the techniques is evaluated using the measures, namely speckle strength index (*SSI*), PSNR index (*PSNR<sub>I</sub>*), correlation preservation index (*CPI*), and entropy (*H*). It may be noted that this measure evaluates the quality of the restored images and does not present any information on the characteristics of the echo-textures. There is no such evidence in the literature describing the

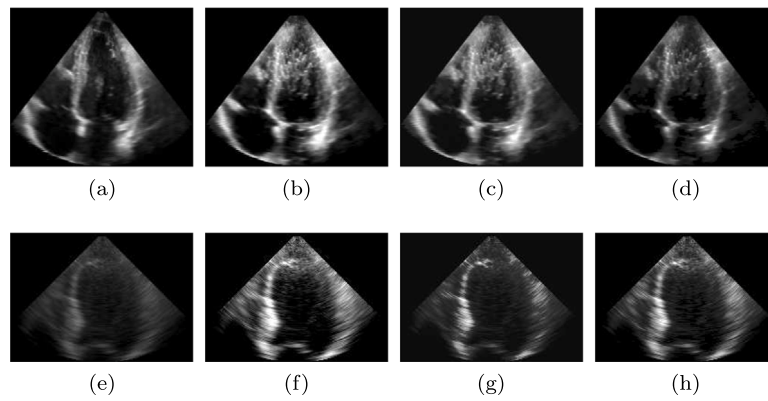


Fig. 8. (a) & (e) Original cardiac slice sample image. Standardized images obtained by: (b) & (f) linear scaling, (d) & (g) Nakagami distribution based histogram specifications and (d) & (h) generalized gamma distribution based histogram specifications.

association of these quantitative measures to the echo-texture. A higher value for the PSNR index and correlation preservation index indicate better performance of the technique. On the contrary, the speckle strength index and entropy are expected to be low in transformed images obtained from the techniques. For computing the measures, let us assume  $y$  to be the input image and  $z$  the transformed image. The measures are computed using Eqs. (15)–(18).

$$SSI = \frac{\sqrt{s_z} \mu_y}{\mu_z \sqrt{s_y}}; \tag{15}$$

where  $\mu_{(\cdot)}$  and  $s_{(\cdot)}$  are the mean and variance of  $z$  and  $y$ .

$$PSNR_I = \frac{\log_{10} \frac{255}{\sqrt{MSE_z}}}{\log_{10} \frac{255}{\sqrt{MSE_y}}}; \tag{16}$$

where

$$MSE_I = \frac{1}{MN} (I - Smooth(I))^2.$$

Here  $I$  is the corresponding image and the  $Smooth(I)$  is its smoothen version. For computation of  $MSE_z$ ,  $I$  is set to  $z$ . If there is no loss in the PSNR value in the transformed image, then PSNR index would be 1. If the PSNR index becomes greater than 1, there is a gain in PSNR and vice versa.

$$CPI = \frac{\omega_{zy}}{\sqrt{s_z} \sqrt{s_y}}; \tag{17}$$

where  $\omega_{zy}$  is the co-variance of  $z$  and  $y$  and  $s_z$  and  $s_y$  are the variance of the image  $z$  and  $y$  respectively. Higher value of CPI indicate better performance of the algorithm.

$$H(I) = - \sum_{i=1}^{255} p_i \log_2 p_i, \tag{18}$$

where

$$p_i = \frac{h_i(I)}{\sum_{k=1}^{255} h_k(I)}. \tag{19}$$

Here,  $h(I)$  is the histogram of image  $I$ .

#### 4.2. Parameters

There are two parameters namely the number of clusters  $K$  and the fuzzifier  $\alpha$ . The number of clusters  $K$  is set to the number of the echo-textures present in the images. As per medical literature [6], echo-texture in ultrasound images can be predominantly grouped into three categories. Hence, we have set the value to 3 in the experiment. The value of fuzzifier  $\alpha$  is set to lie in [1.5, 3). Too small or too large value of the fuzzifier would result in improper characterization of the vagueness in the echo-texture. Thus it is determined experimentally by varying the fuzzifier within the specified range. [24].

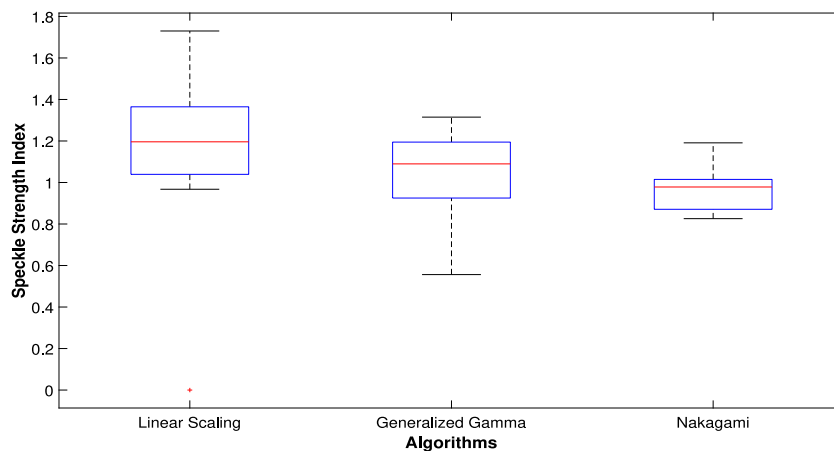
#### 4.3. Linear scaling

Algebraic linear scaling of the image is performed to align the median value of each echo-texture type that remains close to a predefined scope. This predefined range was experimentally determined from a study in [6]. It was found from the study that the median gray value of blood was 0–5, and that of the adventitia was 180–190. Thus, the brightness of all pixels in the image is adjusted according to the linear scale defined by selecting the two reference regions. We have used the same specified range in our experiment.

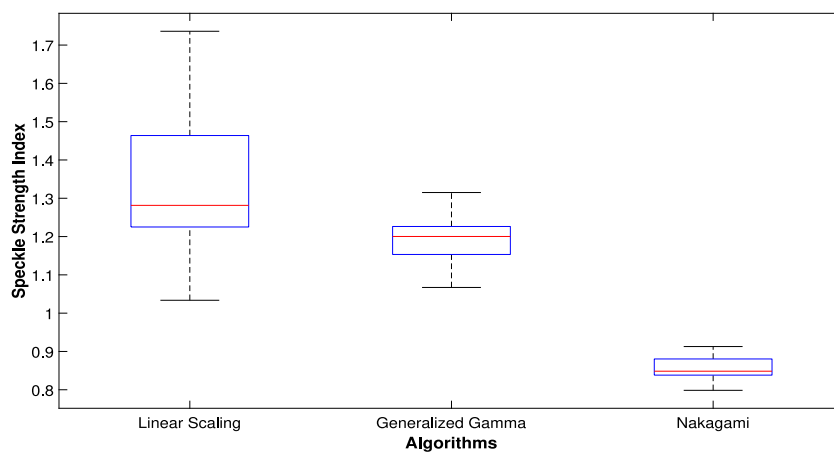
#### 4.4. Result and analysis

Experiments are carried out on three datasets, namely carotid artery, thyroid, and cardiac slice image dataset. The visual results of two test images from each of the three datasets is shown in Figs. 6–8. It is evident from the figures that linear scaling tends to alter the echo-textures as opposed to the proposed histogram specification approach. Moreover, the standardization of the images is not uniform as the gain of the device imposes a bias on the standardization process as opposed to the proposed approach. On comparing the results obtained from the histogram specification with two different distributions, it can be seen that there is a loss of contrast in the results obtained with Nakagami distribution as opposed to a generalized gamma distribution. The generalized gamma distribution preserves the intensities well, especially those belonging to the high echo-texture region. On the contrary, the Nakagami distribution based histogram specification well preserves the low and echogenic echo-texture in the images. It can be evidently seen from Figs. 6(c)–(d).

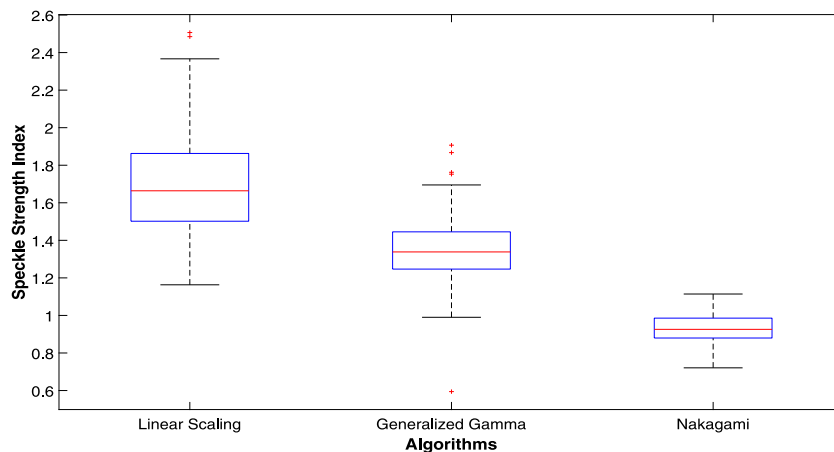
The box plot of five statistics of different measures computed from each of the datasets obtained using different algorithms is shown in Figs. 9–12. It is evident from the figures that linear scaling has a high speckle strength index & entropy, and low PSNR & correlation preservation index. The Nakagami distribution based histogram specification has a low PSNR index except for the thyroid image dataset. This variation is due to the increase in mid-level echo-texture and lowering in hyper echo-texture. Thus a higher entropy is observed for the results obtained from Nakagami distribution based specification. The generalized gamma distribution based histogram specification produces a more stable normalized image as opposed to the others. This findings can be concluded from the entropy value and CPI value provided in Table 2. In fact, the histogram specification-based approach better preserves the correlation in the intensity of the pixels in the standardized image which can be corroborated from the CPI value boxplot shown in Fig. 12. This result is observed because the density of the gray level approximates the non-linear relationships among echo-texture efficiently. Moreover, it could be noticed from the boxplot of



(a)



(b)



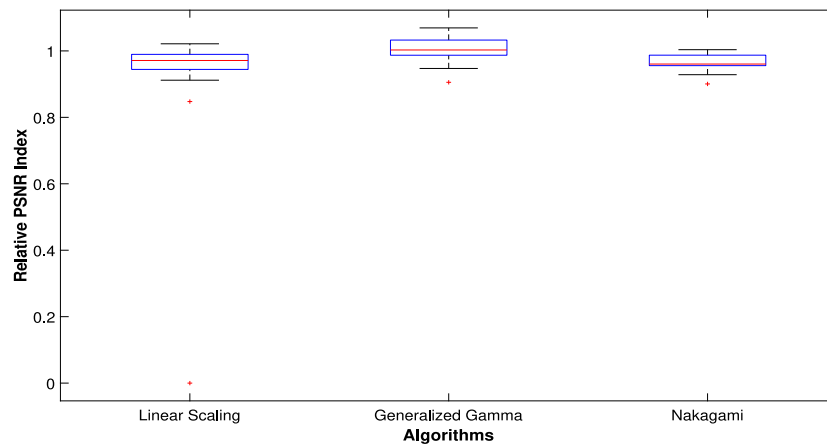
(c)

Fig. 9. Boxplot of speckle strength index of transformed: (a) carotid artery image dataset, (b) cardiac slice image dataset, (c) thyroid image dataset obtained from the standardization techniques.

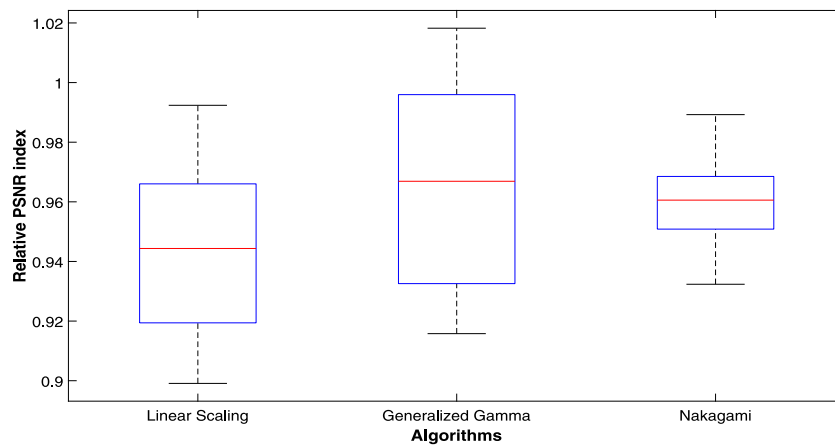
the measures that the inter-quartile range is quite low in the case of a histogram specification-based approach as opposed to the linear scaling. This leads to the conclusion that the proposed histogram specification based standardization approach is not affected by the gain of

the devices. Furthermore, there is a low variance in the results obtained using the proposed technique.

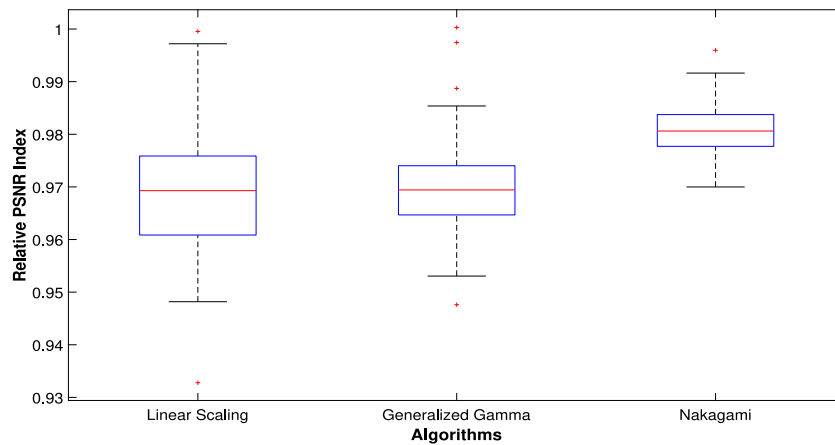
Quantitative results provided in Table 2 also corroborate to the same findings. It can be concluded from the low SSI and high PSNR value that the histogram specification based image standardization



(a)



(b)



(c)

Fig. 10. Boxplot of relative PSNR index: (a) carotid artery image dataset, (b) cardiac slice image dataset, (c) thyroid image dataset.

reduces the noise component in the resultant image. Furthermore, the low entropy value and high CPI observed in the resultant image obtained from the proposed approach over the result obtained from linear scaling confirms the stability of the method.

Some visual changes were noticed in the results obtained from the proposed image standardization approach with different distributions.

However, the average quantitative measure does not reflect much of the significant difference, and both the distributions have more or less similar performance in all the data sets. So it is tough to comment on the choice of distributions at this point of time, and furthermore, the detailed analysis would be needed.

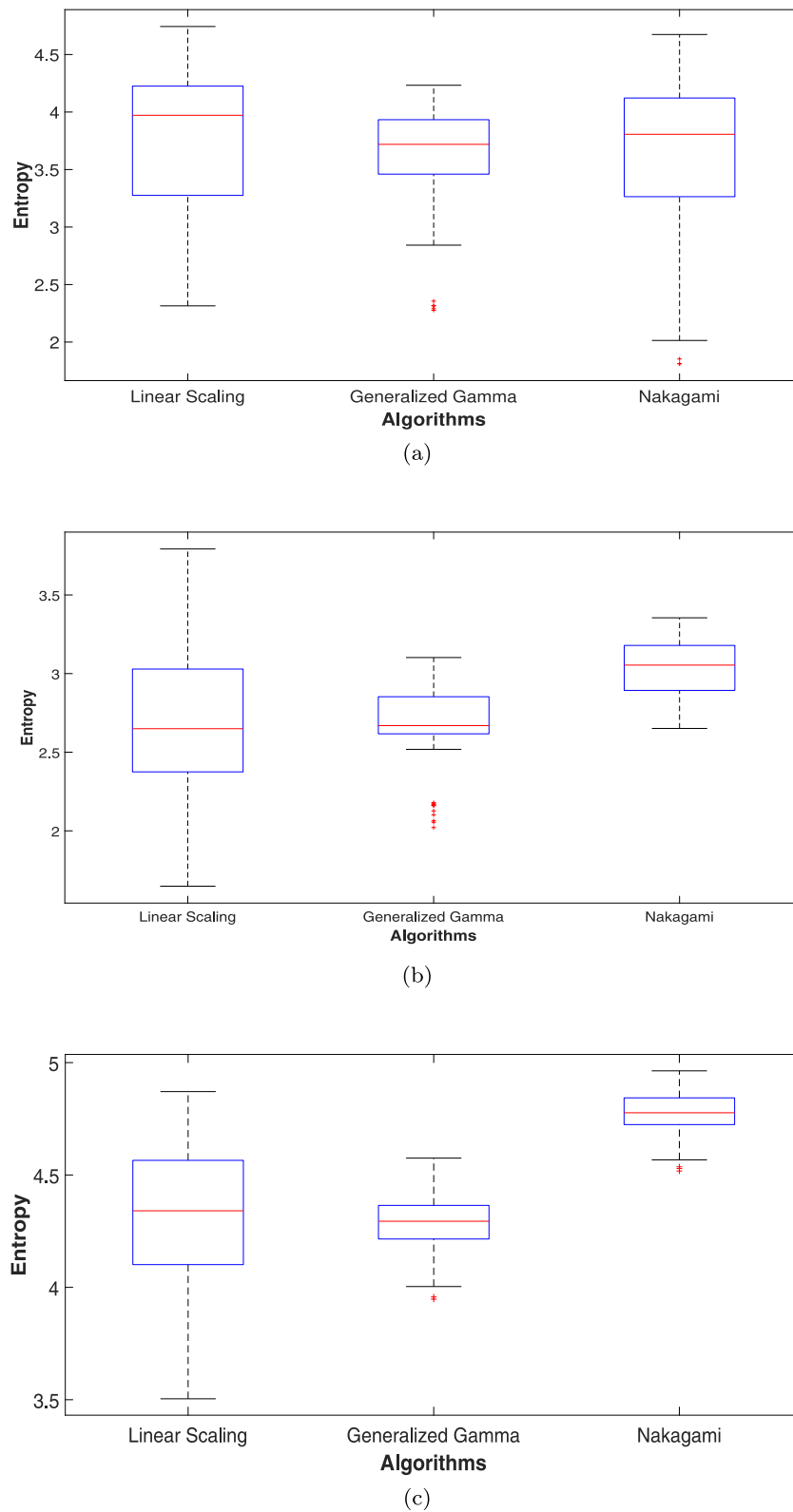


Fig. 11. Boxplot of entropy obtained by the standardization techniques on: (a) carotid artery image dataset, (b) cardiac slice image dataset, (c) thyroid image dataset.

4.5. Discussion

An investigation is made to study the effect of three different kinds of statistics to form the representative parameter set for constructing the reference CDF. The result is shown in Fig. 13. It could be observed that the median set of parameters, provide the best performance as

opposed to the first quartile and mean of the estimated parameters from the representative set. The use of the mean of parameters as a representative for CDF construction increases the entropy of the images and make the transformed image unstable as opposed to the first quartile. On the contrary, the use of the first quartile increases speckle strength. This increase creates a loss of correlation among the

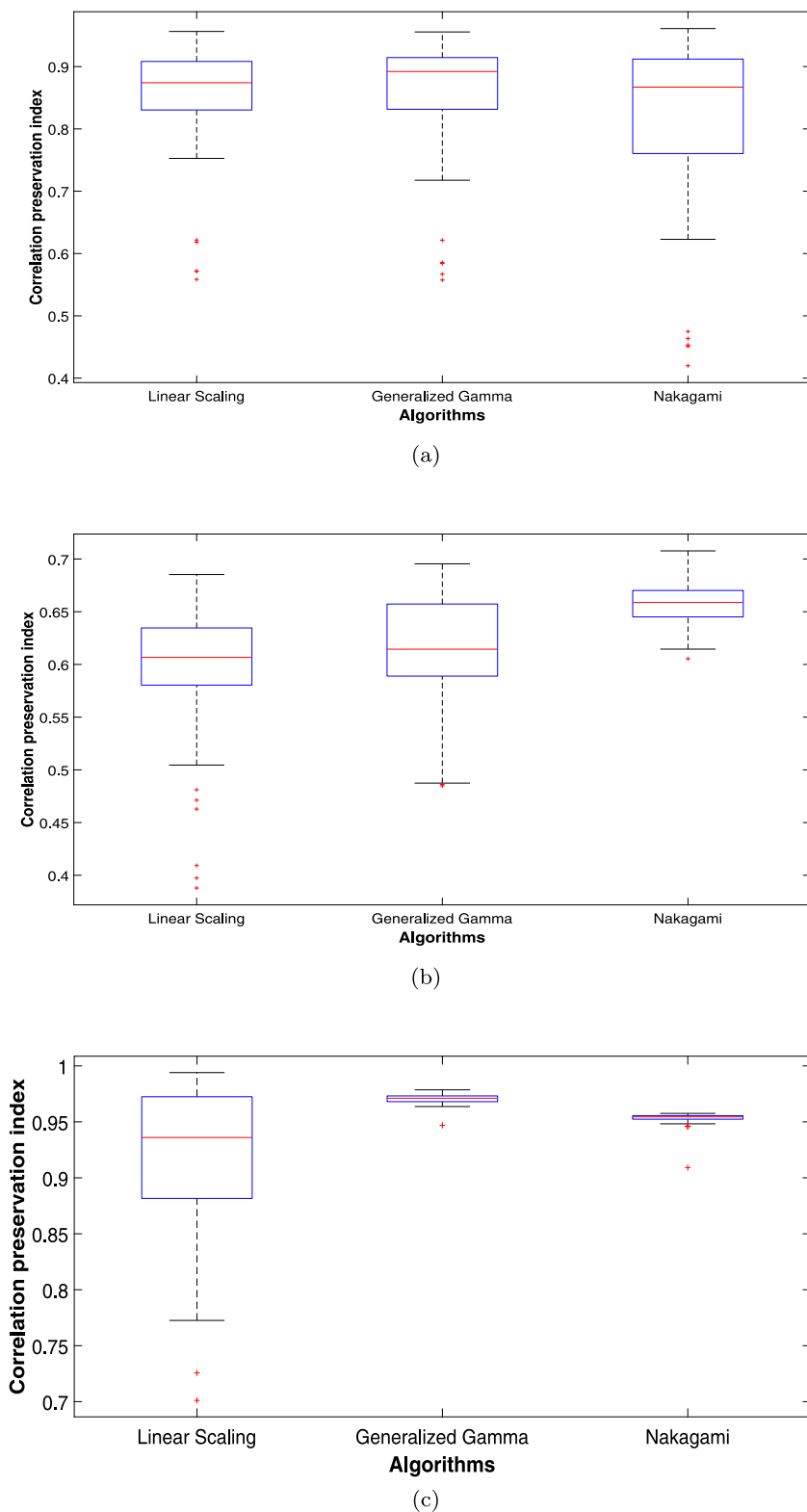


Fig. 12. Boxplot of correlation preservation index obtained by the standardization techniques on: (a) carotid artery image dataset, (b) cardiac slice image dataset, (c) thyroid image dataset.

echo-textures in the images. We also repeated the same experiment for Nakagami distribution based histogram specification, and similar results were observed.

The histogram-based specification better captures the non-linear nature in the echo-texture as opposed to the linear one. So, there is some suppression in speckle strength in the transformed images. Linear

scaling tends to scale the speckle intensity causing an increase in power of the speckle. Moreover, maintaining the non-linearity in the echo-texture helped in preserving the correlation of the gray level in the image. This phenomenon is quite evident from the CPI value presented in Table 2. The use of generalized gamma distribution for construction of reference CDF showed better performance compared to Nakagami

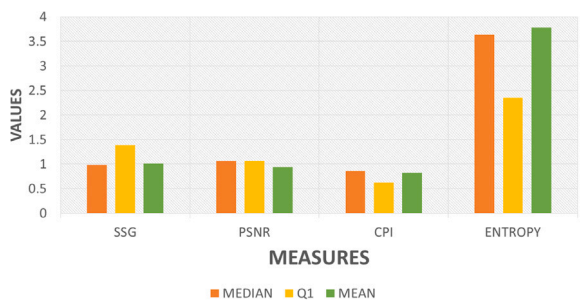


Fig. 13. Effect of different statistics as criteria for parameter estimation for generalized gamma based histogram specification.

distribution. This discrepancy is observed because the Nakagami distribution suffers from a type-II error resulting in the loss of contrast of hyper echo-texture [25]. This results in the low heavy tail and, in turn, error in fitting the hyper echo-texture. Hence, a degradation in the standardization of performance is noticed with Nakagami distribution.

The time required for the initial construction of the prototype parameter is  $O(cmp)$  where  $c$  is the number of echo-textures in a  $m \times n$  image and  $p$  is the number of pictures in the representative image set. This is quite high and makes the process computationally expensive. The computation of the CDF transfer function for image standardization would take  $O(cL)$  computation where  $L$  the number of gray levels in an image and time required for transformation would be  $O(mn)$ . On the contrary, the overall time requirement in linear scaling operations is  $O(mn)$ . Though the total time required for the proposed approach is high for the building of the CDF function, the transformation time of the test image is the same in both the cases. It is noteworthy that the construction time required to build CDF is a one time process and is needed during initialization and update of the system. Thus this could be done offline, and only the transformation is required to be done online. Moreover, the significant gain in the performance for image standardization (as evident from the results) compensate for the increase in time required.

## 5. Conclusion

A histogram specification based ultrasound image standardization approach is presented in this article. A transfer function is formed for histogram specification by finding the CDF with a prototype parameter set and distribution functions, which characterizes each echo-texture. The prototype parameter set is constructed by selecting suitable representatives from the parameters determined from the representative images. The obtained transfer function is used for standardizing the input image. The proposed approach is also invariant to change in scale and size of the images used for standardization.

The designed standardization approach is tested on ultrasound images of several organs, and it observed it better retains the non-linear relationship among the echo-textures as compared to the linear one and preserves the correlation among the echo-textures. It can be seen from the results that histogram specification based standardization has better stability. The use of generalized gamma for construction of transfer function provided better balance and also preserved the correlation among the echo-textures. On the contrary, the use of Nakagami distribution provided better speckle suppression in the standardized image.

The proposed approach could be further enhanced if spatial information is taken into consideration while designing the transfer function. This enhancement would help in performing further standardization and speckle suppression simultaneously.

The time required for the proposed approach is higher compared to the linear scaling approach. Nonetheless, the proposed method also produces a stable image as opposed to the linear scaling approach.

## Declaration of competing interest

No author associated with this paper has disclosed any potential or pertinent conflicts which may be perceived to have impending conflict with this work. For full disclosure statements refer to <https://doi.org/10.1016/j.combiomed.2020.103746>.

## Acknowledgments

This work was supported by the Department of Electronics and Information Technology (DEITY), Government of India under Visvesvaraya Ph.D. Scheme for Electronics and IT [PhD/MLA/4(90)/2015-16] and Department of Science and Technology, Government of India under Interdisciplinary Cyber-Physical System (ICPS) programme.

## References

- [1] D. Mittal, V. Kumar, S.C. Saxena, N. Khandelwal, N. Kalra, Enhancement of the ultrasound images by modified anisotropic diffusion method, *Med. Biol. Eng. Comput.* 48 (12) (2010) 1281–1291.
- [2] Y. Wang, H. Peng, C. Zheng, Z. Han, H. Qiao, A dynamic generalized coherence factor for side lobe suppression in ultrasound imaging, *Comput. Biol. Med.* 116 (2020) 103522.
- [3] K.M. Meiburger, U.R. Acharya, F. Molinari, Automated localization and segmentation techniques for B-mode ultrasound images: A review, *Comput. Biol. Med.* 92 (2018) 210–235.
- [4] M. Ciecholewski, An edge-based active contour model using an inflation/deflation force with a damping coefficient, *Expert Syst. Appl.* 44 (2016) 22–36.
- [5] M. Ciecholewski, J. Chochołowicz, Gallbladder shape extraction from ultrasound images using active contour models, *Comput. Biol. Med.* 43 (12) (2013) 2238–2255.
- [6] T. Elatrozy, A. Nicolaides, T.H. Tegos, A.Z. Zarka, et al., The effect of B-mode ultrasonic image standardisation on the echodensity of symptomatic and asymptomatic carotid bifurcation plaques, *Int. Angiol.* 17 (3) (1998) 179–186.
- [7] C.P. Loizou, C.S. Pattichis, M. Pantziaris, T. Tyllis, A. Nicolaides, Quality evaluation of ultrasound imaging in the carotid artery based on normalization and speckle reduction filtering, *Med. Biol. Eng. Comput.* 44 (5) (2006) 414–426.
- [8] C.P. Loizou, C.S. Pattichis, M. Pantziaris, T. Tyllis, A. Nicolaides, Snakes based segmentation of the common carotid artery intima media, *Med. Biol. Eng. Comput.* 45 (1) (2007) 35–49.
- [9] R.C. Gonzales, R.E. Woods, *Digital Image Processing*, Prentice hall New Jersey, 2002.
- [10] G.J. Klir, B. Yuan, *Fuzzy Sets and Fuzzy Logic: Theory and Applications*, Pearson Education, India, 2015.
- [11] A. Ghosh, S.K. Pal, *Soft Computing Approach to Pattern Recognition and Image Processing*, volume 53, World Scientific, 2002.
- [12] A. Ghosh, Use of fuzziness measures in layered networks for object extraction: a generalization, *Fuzzy Sets and Systems* 72 (3) (1995) 331–348.
- [13] P.M. Shankar, A general statistical model for ultrasonic backscattering from tissues, *IEEE Trans. Ultrason. Ferroelectr. Freq. Control* 47 (3) (2000) 727–736.
- [14] G. Vegas-Sanchez-Ferrero, S. Aja-Fernandez, C. Palencia, M. Martin-Fernandez, A generalized gamma mixture model for ultrasonic tissue characterization, *Comput. Math. Methods Med.* 2012 (2012) 1–25.
- [15] O.V. Michailovich, A. Tannenbaum, Despeckling of medical ultrasound images, *IEEE Trans. Ultrason. Ferroelectr. Freq. Control* 53 (1) (2006) 64–78.
- [16] R.M. Rangayyan, *Biomedical Image Analysis*, CRC press, 2004.
- [17] P.M. Shankar, A general statistical model for ultrasonic backscattering from tissues, *IEEE Trans. Ultrason. Ferroelectr. Freq. Control* 47 (3) (2000) 727–736.
- [18] O. Gomès, C. Combes, A. Dussauchoy, Parameter estimation of the generalized gamma distribution, *Math. Comput. Simulation* 79 (4) (2008) 955–963.
- [19] T.H. Wonnacott, R.J. Wonnacott, *Introductory Statistics*, volume 5, Wiley New York, 1990.
- [20] C.P. Loizou, C.S. Pattichis, Despeckle filtering of ultrasound images, in: J.S. Suri, C. Kathuria, F. Molinari (Eds.), *Atherosclerosis Disease Management*, Springer New York, 2011, pp. 153–194.
- [21] K. Riha, J. Masek, R. Burget, R. Benes, E. Zavodna, Novel method for localization of common carotid artery transverse section in ultrasound images using modified Viola-Jones detector, *Ultrasound Med. Biol.* 39 (10) (2013) 1887–1902.
- [22] O. Bernard, J.G. Bosch, B. Heyde, M. Alessandrini, D. Barbosa, S. Camarasu-Pop, F. Cervenansky, S. Valette, O. Mirea, M. Bernier, et al., Standardized evaluation system for left ventricular segmentation algorithms in 3D echocardiography, *IEEE Trans. Med. Imaging* 35 (4) (2016) 967–977.
- [23] L. Pedraza, C. Vargas, F. Narvaez, O. Duran, E. Munoz, E. Romero, An open access thyroid ultrasound image database, *Proc. SPIE - Int. Soc. Opt. Eng.* 9287 (2015) 92870W–92870W–6.
- [24] R. Roy, S. Ghosh, A. Ghosh, Speckle de-noising of clinical ultrasound images based on fuzzy spel conformity in its adjacency, *Appl. Soft Comput.* 73 (2018) 394–417.
- [25] P.M. Shankar, Ultrasonic tissue characterization using a generalized Nakagami model, *IEEE Trans. Ultrason. Ferroelectr. Freq. Control* 48 (6) (2001) 1716–1720.



**Rahul Roy** received the M. Tech in Computer science and Engineering from KIIT University, Odisha, India in 2011 and Integrated M.Sc in Computer Science from Assam University, Assam, India, in 2009. He is presently pursuing Ph.D in Computer Science and Engineering from Jadavpur University and is working as assistant professor in National Institute of Science and Technology. His current research interest includes biomedical image analysis, machine learning, data analytics and computational intelligence.



**Susmita Ghosh** received the B.Sc. (with honors) in Physics and the B.Tech. in Computer Science and Engineering from the University of Calcutta, India, in 1988 and 1991, respectively, the M.Tech. in Computer Science and Engineering from the Indian Institute of Technology, Bombay, in 1993, and the Ph.D. (Engineering) from Jadavpur University, Kolkata, in 2004. She has visited various universities/academic institutes for collaborative research/ international projects and delivered lectures in different countries including Australia, China, Italy, Japan and the USA. She has published many research papers in internationally reputed journals and referred conferences and has edited 3 books. She was a Lecturer and then a Reader with the Department of Computer Science and Engineering, Jadavpur University since 1997. She is currently an Associate Professor at the same department. Her research interests include genetic algorithms, neural networks, image processing, pattern recognition, soft computing, and remotely sensed image analysis.



**Ashish Ghosh** is a professor at the Machine Intelligence Unit, Indian Statistical Institute. He has already published more than 170 research papers in internationally reputed journals and refereed conferences, and has edited eight books. His current research interests include Pattern Recognition and Machine Learning, Deep Learning, Data Mining, Big Data Analysis, Image Analysis, Remotely Sensed Image Analysis, Video Image Analysis, Soft Computing, Fuzzy Sets and Uncertainty Analysis, Neural Networks, Evolutionary Computation, and Bioinformatics. Dr. Ghosh received the prestigious and most coveted Young Scientists Award in Engineering Sciences from the Indian National Science Academy in 1995, and in Computer Science from the Indian Science Congress Association in 1992. He was selected as an Associate of the Indian Academy of Sciences, Bangalore, India, in 1997. He is a member of the founding team that established the National Center for Soft Computing Research at the Indian Statistical Institute, Kolkata, in 2004, with funding from the Department of Science and Technology, Government of India, and is currently the In-charge of the Center. He is acting as a member of the editorial boards of various international journals.